2018 22nd International Conference on System Theory, Control and Computing (ICSTCC)

Experimental Validation of Quadrotors Angular Stability in a Gyroscopic Test Bench

M. F. Santos*, M. F. Silva†, V. F. Vidal‡,
L. M. Honório§, V. L. M. Lopes ¶, L. A. Z. Silva ‖, H. B. Rezende**,
J. M. S. Ribeiro ††, A. S. Cerqueira‡‡, A. A. N. Pancoti[x], B. A. Regina[xi]

Centro Federal de Educação Tecnológica de Minas Gerais,
CEFET-MG, Leopoldina, MG, 36700-000, Brazil
murillo@leopoldina.cefetmg.br*

Juiz de Fora Federal University,
UFJF, Juiz de Fora, MG, 36036-900, Brazil
mathausfsilva@hotmail.com†, vinicius.vidal@engenharia.ufjf.br‡, leonardo.honorio@ufjf.edu.br§,
vmainenti@gmail.com¶, luiz.zillmann@engenharia.ufjf.br‖, henrique.rezende@engenharia.ufjf.br**,
joao.ribeiro@engenharia.ufjf.br††, augusto.santiago@ufjf.edu.br‡‡, antonio.pancoti@engenharia.ufjf.br[x],
almeida.bruno@engenharia.ufjf.br[xi]

***Abstract*—This work presents a gyroscopic test bench for under or over-actuated UAVs. In this way, it is possible to perform stability tests and several control loop structures without taking the risk of damages present in field tests, or even accidents with personal injuries. Moreover, the vehicle continues with its respective degrees of freedom for angular stability dynamics (rolling, pitching and yawing), without (or almost no) interference from the test bench, as it does not influence the UAV moments of inertia. It also can be used for didactic purposes, where, through the results presented in graphics and videos, it proved to be easy to build and handled, meeting the minimum safety requirements proposed.**

***Keywords*—UAV, Didactic System, Test Bench Platform.**

I. Introduction

Nowadays, Unmanned Aerial Vehicles (UAV) have widespread over the world, being considered in several commercial tasks such as surveillance, ground mapping, agricultural and environmental preservation practices, fire detection, transmission power line infra-red supervision, among others [1], [2].

There are several UAV topologies, classified as fixed-wings (planes), rotary wings (helicopters and multicopters) and other hybrid categories (balloons and airships). Each of these airframe configurations has advantages and disadvantages depending on the design specifications and applications.

After concluding a UAV project, it is indispensable to perform tests and evaluate its controlled response, such as auditing its control loops to check if it reached the project requirements.

One possible way to do that is considering test bench platforms. Researches on the Internet depict some choices, sometimes not practical or safe. Then, it reaffirms the necessity of creating a safe and reliable test bench system.

Taking quadcopter topologies into account, this work aims to present the development of a gyroscopic test bench platform for some UAV topologies (respecting its dimension requirements). Through this apparatus, it is possible to analyze UAV angular stability in 3 degrees of freedom (rolling, pitching and yawing), enabling to validate tests with different control algorithms, signal estimation techniques, such as other preliminaries and previous attempts. It can also be perfectly used as an educational environment for academic purposes.

This paper is organized as follows: Section II presents the aircraft features, used as a tool in this work; Section III shows some related works where were presented didactic test benches for UAV angular stability validation; Section IV depicts the gyroscopic platform created and performed in this work, with all its constructive characteristics; Section V describes the full kinematics and dynamics modeling of the quadcopter UAV; Section VI presents the simulation results obtained in this work; Section VII concludes this purpose, such as some notes; Section VIII lectures about future works enabled to develop after the conclusion of this gyroscope test bench platform.

II. Aircraft Developed

Initiating the description of the components by the propulsion system, 4 brushless motors of Scorpion M-2205-2350KV type, 4 King-Kong 5x4P propellers and 4 Electronic Speed Controllers (ESC) (Q-Brain 4 x 25A SBEC) were used.

Thus, given the propulsion system chosen and the total aircraft weight ($1Kg$), the projected payload is estimated to be approximately $0.55Kg$ according to the experimental bench tests performed.

About power supply, it was used a LiPO (Lithium-Polymer) battery with 3 cells, 11.1V, 4000mAh, 25C, with the commitment of low weight, high payload and immediate current discharge (if necessary). This battery allows the UAV an autonomy between 20 and 25 minutes of flight.

Concerning about programming language, it was chosen C++, implemented in a microcontroller type 168 MHz 32 Bits Arm Cortex M4F, embedded in a specific platform created for UAVs, named by Pixhawk.

To filter the noises, it was developed Low-Pass Filters with their respective cut-off frequencies of each control loop, embedded in the UAV control board.

The UAV inertia matrix ($\boldsymbol{I_{CG}} \in \mathbb{R}^{3\times3}$) is expressed below:

$$\begin{aligned} \boldsymbol{I_{CG}} &= \begin{bmatrix} I_x & -I_{xy} & -I_{xz} \\ -I_{xy} & I_y & -I_{yz} \\ -I_{xz} & -I_{yz} & I_z \end{bmatrix} \\ &= \begin{bmatrix} 4456688.30 & 18.23 & -451.92 \\ 18.23 & 6827331.63 & 21814.62 \\ -451.92 & 21814.62 & 3393152.46 \end{bmatrix} \end{aligned} \quad (1)$$

where $\boldsymbol{I_{CG}} \in \mathbb{R}^{3x3}$ is the UAV inertia matrix, expressed in $g.mm^2$.

Fig. 1 depicts the aircraft used in this work to validate the gyroscopic test bench, proposed here.

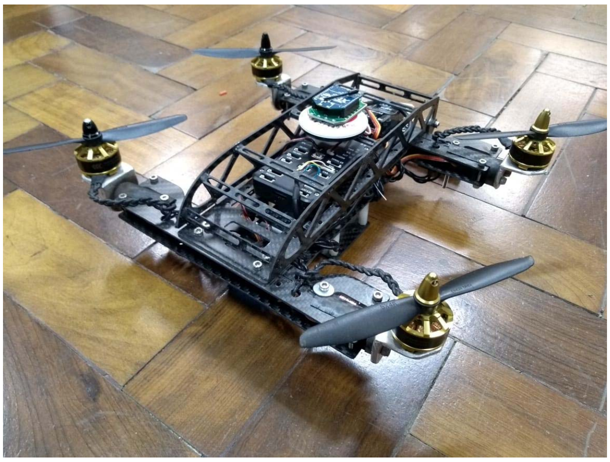

Figure 1. Aircraft used in this work to validate the gyroscopic test bench.

III. Related Platforms

A quick research on the Internet can show some platforms for testing UAV angular stability, even in rudimentary forms. It is also possible to observe how vital these test benches are for the whole UAV project, due to its preliminary tests before outdoors field experiments.

Some rudimentary devices for aircraft control experimental tests can also be easily found. About test bench structures of UAVs, it is most of the time composed of only one rope/elastic object, preventing it from touching the ground, i.e., limiting space of reach if an unexpected behaviour happens.

Sometimes, others have rigid, articulated and single-axis supports, enabling only one degree of freedom for the vehicle. Moreover, the articulated support for only one axis has the limitation of not being able to analyze the responses of the controllers together, much less when this action interferes in another degree of freedom.

Approaching the structure with a rope that fixes/limits the UAV space of work, there is a whole risk for the rotors to get tangled in the support, being able to cause an accident. Moreover, if the complete loss of the UAV stability is observed, it can generate accelerations due to the rope limits, also causing damage to the aircraft or injuries to people. Another disadvantage of this method is the insertion of the ground effect caused by the elasticity of the rope, even if it is not extensible. Then, it inserts into the system behaviour that is not characteristic of UAVs.

Some related works which concern to test bench platform can be mentioned. Works [3] and [4] proposed a system for testing light vertical UAVs take-off and landing, named by them as "DronesBench". This system aims to detect fault related to the RPAS components by measuring the thrust force control action, the power consumption, and the attitude stability. They showed some preliminary results using a quadcopter vehicle. Regarding the conclusions, they considered it was satisfactory and consistent with platforms found nowadays. It is important to highlight the considerable size of the proposed platform, as well as some particularities necessary to conduct tests in 3 degrees of freedom.

The authors in work [5] developed a low-cost quadcopter prototype intended as a research platform to study control algorithms for autonomous flights. They created two test bench systems, where the first one was done to observe the quadcopter behaviour in 3 degrees of freedom (rolling, pitching and yawing). It consists of a series of concentric bases with bearings which allows the vehicle rotates freely. With concerns to the second test bench, the aircraft was coupled with ropes to the roof and the ground inside a closed place. They considered the results satisfactory saying that the test benches did not interfere in UAV dynamics controlled responses. However, it can be highlighted that the presence of ropes can add elastic effects to the system through Hooke's law.

Another notable work is developed by the authors in [6]. They built a low-cost quadcopter to identify and analyze its dynamics modelling through 2 test bench systems. The first one has 3 degrees of freedom that allows the aircraft to rotate while retaining translation movements. The second one has only 1 degree of freedom, which indeed allows it to obtain the UAV center of gravity. At last, the test benches were used to identify the actuator parameters and the UAV inertia moments. They mentioned the success of its implementation, advising some possible future improvements in their project.

IV. Test Bench Platform

For the accomplishment of the experimental tests for 3 degrees of freedom, a gyroscopic test bench was developed serving as a safe environment for aircraft experiments and simulation.

With this structure, angular stability tests and various control structures can be analyzed without taking the risk of damages present in the field tests, or even accidents with personal injuries. Moreover, the vehicle maintains with its respective degrees of freedom for angular stability dynamics (rolling, pitching, and yawing), without (or almost no) interference from the gyroscopic platform, proposed here also for educational purposes.

The platform is composed of gyroscopic support articulated in three axes of rotation, where the vehicle is coupled. The support consists of a base where a ring-shaped structure is fastened employing shafts and bearings (with almost zero friction), and finally attached to a pivotal coupling, serving as the basis for the UAV placement.

The gyroscopic platform dimensions were designed to allow the vehicle to rotate in all directions without colliding with another piece of it, operating freely. The central support (a part that is inside the ring of the support) has a slightly lowered recess, which allows placing the UAV gravity center at a height lower than the gyroscopic base rotation axis.

It leads the system to be stable, making it function as a simple pendulum, returning to its resting position. However, it is possible to regulate this height by adjusting and moving the location of the system gravity center entirely. It also allows to create a marginally stable condition (center of gravity position coinciding with the rotation axis) or unstable (center of gravity above the system rotation axis, operating as an inverted pendulum). This possibility permits users to observe and manipulate the behavior of these three types of under or over-actuated UAVs in unfavorable conditions, exemplifying an unstable vehicle.

Some illustrations of the developed platform are shown in Figure 2.

The indices of Fig. 2c are: 1-Base; 2-Axis between the base and the ring of the gyroscope; 3-Axis between the gyroscope ring and the rotation bar; 4-Rotation bar; 5-Bearings; 6-Fixing ring; 7-Axis between the rotation bar and the base of UAV fixation; 8-Base of vehicle fixation; 9-Gyroscopic ring.

As for the structure weight, its total mass was of $0.994Kg$, being made with low-density wood, occupying $548950.7379mm^3$. Further illustrations of the developed platform are shown in Fig. 3, where some size information are quoted.

V. Aircraft Kinematics and Dynamics Modeling

Prior to present the full aircraft modeling, it is necessary to describe the state variables. The vector $[p_n, p_e, h]^T$ represents the inertial North, East and Altitude (facing down) positions along the $(\hat{i}^i, \hat{j}^i, -\hat{k}^i)$ axes representing the inertial frame $(\mathcal{F}^I)$; the vector $[\phi, \theta, \psi]^T$ represents the roll, pitch and yaw angles considering the vehicle frame $(\hat{i}^v, \hat{j}^v, -\hat{k}^v)$. The vectors $[u, v, \omega]^T$ and $[p, q, r]^T$ represent the three dimensional speeds and angular velocities over the axes $(\hat{i}^b, \hat{j}^b, -\hat{k}^b)$ of the body frame $(\mathcal{F}^b)$ [7], [8].

The UAV position $\boldsymbol{\eta} \in \mathbb{R}^6$ is the generalized position with vector $\boldsymbol{\eta_1} \in \mathbb{R}^3$ between origins of $\mathcal{F}^I$ and $\mathcal{F}^b$, while $\boldsymbol{\eta_2} \in \mathbb{R}^3$ is defined with the orientation of $\mathcal{F}^b$ with the respect to the $\mathcal{F}^I$. The orientation is defined with three consecutive rotations around the $\mathcal{F}^I$ coordinate axes, roll-pitch-yaw order. According to [9], (2) presents the default nomenclature.

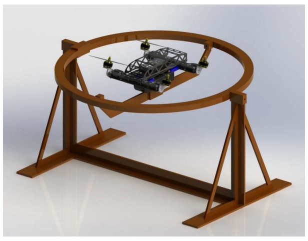

(a) Illustrative picture of the gyroscopic test bench system on *software SolidWorks®*.

(b) Illustrative picture of the gyroscopic test bench system after its assembly with a quadrotor UAV.

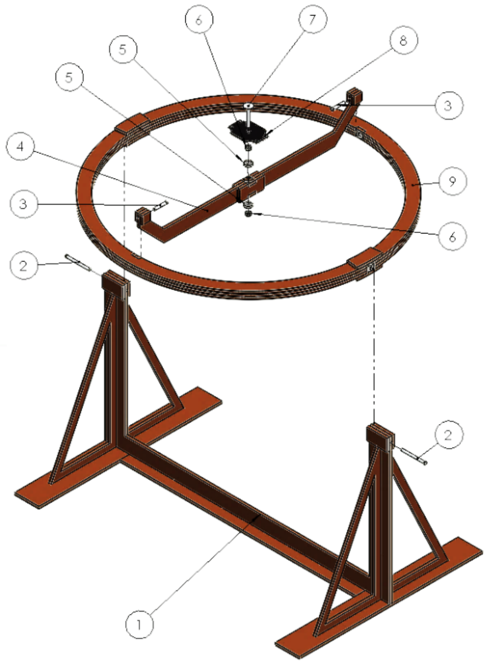

(c) Exploded view of the gyroscopic test bench on *software SolidWorks®*.

Figure 2. Illustrative picture of the developed platform.

$$\begin{aligned} \boldsymbol{\eta_1} &= [p_n \quad p_e \quad h]^T \\ \boldsymbol{\eta_2} &= [\phi \quad \theta \quad \psi]^T \\ \boldsymbol{\eta} &= [\boldsymbol{\eta_1} \quad \boldsymbol{\eta_2}]^T \end{aligned} \tag{2}$$

Regarding to velocities, (3) presents them:

$$\begin{aligned} \boldsymbol{\nu_1} &= [\boldsymbol{v^b}] = [u \quad v \quad w]^T \\ \boldsymbol{\nu_2} &= [\boldsymbol{\omega^b}] = [p \quad q \quad r]^T \\ \boldsymbol{\nu} &= [\boldsymbol{\nu_1} \quad \boldsymbol{\nu_2}]^T \end{aligned} \tag{3}$$

where $\boldsymbol{\nu} \in \mathbb{R}^6$ is the generalized velocity vector, $\boldsymbol{\nu_1} \in \mathbb{R}^3$ is the linear velocity vector, $\boldsymbol{\nu_2} \in \mathbb{R}^3$ is the angular velocity vector, both in $\mathcal{F}^b$.

The 6 Degrees of Freedom (DOFs) rigid body kinematics and dynamics model is expressed in Equation 4.

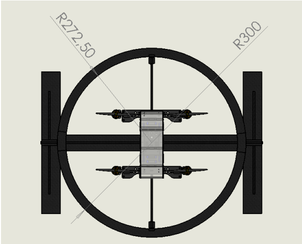

(a) Gyroscope plaftorm top view on *software* $SolidWorks^{®}$.

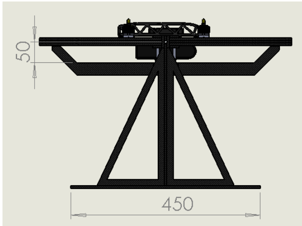

(b) Gyroscope plaftorm lateral view on *software* $SolidWorks^{®}$.

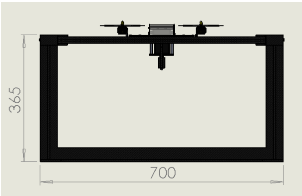

(c) [Gyroscope plaftorm front view on *software* $SolidWorks^{®}$.

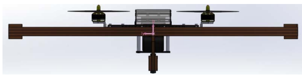

(d) Gyroscope platform front view, leveled to the UAV vehicle on *software* $SolidWorks^{®}$.

Figure 3. Main views fo the gyroscopic test bench developed.

$$\dot{\boldsymbol{\eta}} = \boldsymbol{J}\boldsymbol{\nu} \tag{4}$$

where $\dot{\boldsymbol{\eta}} \in \mathbb{R}^6$ is the generalized velocity vector in $\mathcal{F}^I$ and $\boldsymbol{J} \in \mathbb{R}^{6\times6}$ is the generalized rotation and transformation matrix, presented below:

$$\boldsymbol{J} = \begin{bmatrix} \boldsymbol{J_1} & \boldsymbol{0_{3\times3}} \\ \boldsymbol{0_{3\times3}} & \boldsymbol{J_2} \end{bmatrix} \tag{5}$$

$$\boldsymbol{J_1} = \begin{bmatrix} c\theta c\psi & s\phi s\theta c\psi - c\theta s\psi & c\phi s\theta c\psi + s\phi s\psi \\ c\theta s\psi & s\phi s\theta s\psi + c\phi c\psi & c\phi s\theta s\psi - s\phi c\psi \\ -s\theta & s\phi c\theta & c\phi c\theta \end{bmatrix} \tag{6}$$

$$\boldsymbol{J_2} = \begin{bmatrix} 1 & s\phi t\theta & c\phi t\theta \\ 0 & c\phi & -s\phi \\ 0 & s\phi c\theta & c\phi c\theta \end{bmatrix} \tag{7}$$

where $c\theta \triangleq \cos\theta$, $s\theta \triangleq \sin\theta$, $t\theta \triangleq \tan\theta$, $\boldsymbol{J_1} \in \mathbb{R}^{3\times3}$ is the rotation matrix to relate linear velocity vector and $\boldsymbol{J_2} \in \mathbb{R}^{3\times3}$ is the rotation matrix to relate angular velocity vector, both from $\mathcal{F}^b$ to $\mathcal{F}^I$.

Differential equations describe UAV dynamics from the Newton-Euler method. The 6 DOFs rigid body takes into consideration the mass m and the inertia of the body $\boldsymbol{I_{CG}}$, as shown in (8).

$$\boldsymbol{M_b}\dot{\boldsymbol{\nu}} + \boldsymbol{C_b}(\boldsymbol{\nu})\boldsymbol{\nu} = \boldsymbol{\tau} \tag{8}$$

where:

$$\boldsymbol{M_b} = \begin{bmatrix} m\boldsymbol{I} & \boldsymbol{0_{3\times3}} \\ \boldsymbol{0_{3\times3}} & \boldsymbol{I_{CG}} \end{bmatrix} \tag{9}$$

$$\boldsymbol{C_b}(\boldsymbol{\nu}) = \begin{bmatrix} m\boldsymbol{S}(\boldsymbol{\nu_2}) & \boldsymbol{0_{3\times3}} \\ \boldsymbol{0_{3\times3}} & -\boldsymbol{S}(\boldsymbol{I_{CG}}\boldsymbol{\nu_2}) \end{bmatrix} \tag{10}$$

$$\boldsymbol{\tau} = \boldsymbol{\tau^p} + \boldsymbol{\tau^g} \tag{11}$$

where $\boldsymbol{M_b} \in \mathbb{R}^{6\times6}$ is the system inertia matrix, $\boldsymbol{C_b}(\boldsymbol{\nu}) \in \mathbb{R}^{6\times6}$ is the Coriolis-centripetal matrix, at the body-fixed frame $\mathcal{F}^b$, $\boldsymbol{S}(\boldsymbol{\nu_2}) \in \mathbb{R}^{3\times3}$ is the skew-symmetrical matrix of vector $\boldsymbol{\nu_2}$, $\boldsymbol{\tau} \in \mathbb{R}^6$ is resultant vector compound by Gravitational $\boldsymbol{\tau^g} \in \mathbb{R}^6$ and Propulsion $\boldsymbol{\tau^p} \in \mathbb{R}^6$ forces and torques, both in the body-fixed frame $\mathcal{F}^b$. Note that $\boldsymbol{I} \in \mathbb{R}^{3\times3}$ is the identity matrix, different from $\boldsymbol{I_{CG}}$.

More details about the modelling and control loops considered in this work can be found in [10], [11]. Details of the UAV features are presented in the works [2], [12]–[14], where the same aircraft and methodology was considered.

VI. Experimental Results

The experimental results presented in this work are divided into 4 different scenarios, each one representing at least one aircraft degree of freedom with different SetPoint (SP) signals.

It is important to highlight that the aircraft was not projected in the current work, it was only used as a tool to validate the gyroscopic test bench.

The experimental tests were performed in a quiet and calm environment, where it is possible to eliminate wind disturbances.

Concerning the vehicle battery voltage, it was always kept charged up to at least 75%, avoiding electrical system low efficiency.

Before presenting these scenarios, a video was made and uploaded on YouTube showing random maneuvers from the pilot radio controller, in all 3 quadrotor UAV dynamics (rolling, pitching, and yawing). The video is available on YouTube through the link https://youtu.be/AbV90z-rbY8.

A. Scenario 1

The first scenario was created to show maneuvers in 2 dynamics at the same time, roll and yaw angular positions. The controlled response in the developed test bench can be seen in Fig. 4

As it is possible to see from the previous figure, the rolling and yawing SPs were requested at the same time in 2 situations, 2 positive SPs and, in the end, 2 negative ones. The UAV performed the SPs satisfactorily, evaluating the test bench system. To exemplify the results presented here, a video was uploaded on YouTube: https://youtu.be/2f8zut5luB0.

B. Scenario 2

The second scenario is also presented to show 2 maneuvers in 2 dynamics at the same time, but now for pitch and yaw angular attitudes. Figure 5 depicts the controlled responses.

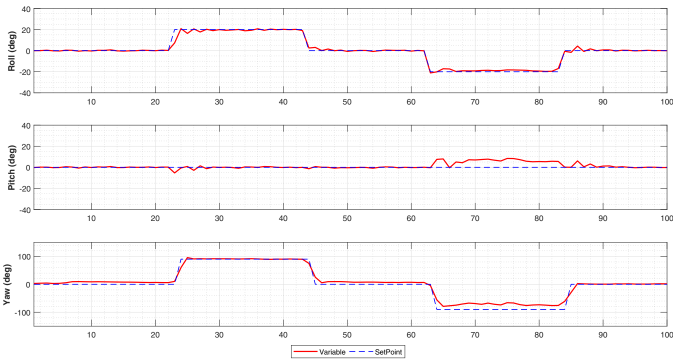

Figure 4. Angular attitude controlled responses performed in Scenario 1.

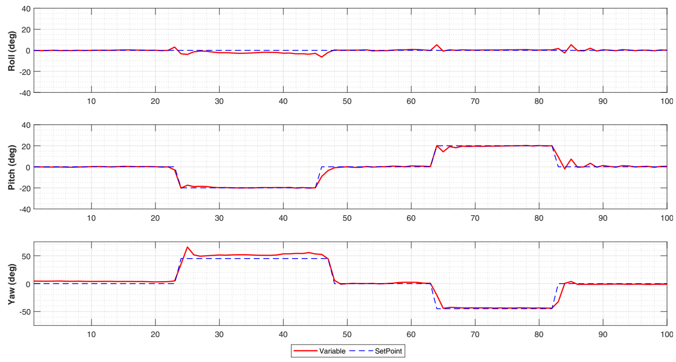

Figure 5. Angular attitude controlled responses performed in Scenario 2.

Here again, an UAV stable behaviour is observed where 2 SPs were requested at the same time, showing that the proposed platform worked reasonably. A second video was made for this scenario, also available on YouTube: https://youtu.be/EqX5oAQtpWg.

C. Scenario 3

For this scenario, it is shown the UAV behavior when 3 SPs were done at the same time. It is a critical situation when analyzing UAV angular stability, because experimental field tests always demand firm control action, even from wind disturbance or by autonomous missions.

Figure 6 presents the angular attitude controlled responses for rolling, pitching and yawing.

This scenario was the hardest flight condition requested to be done by the aircraft. As it is seen, the test bench platform allowed the UAV to do the maneuvers freely. To illustrate this scenario, it was uploaded on YouTube this experimental test: https://youtu.be/L1lCX3EBFVQ.

D. Scenario 4

This last scenario is important to show yaw velocity stability, where the others 2 dynamics (rolling and pitching) were maintained at 0 degrees during the whole experiment test. Figure 7 illustrates the UAV controlled responses.

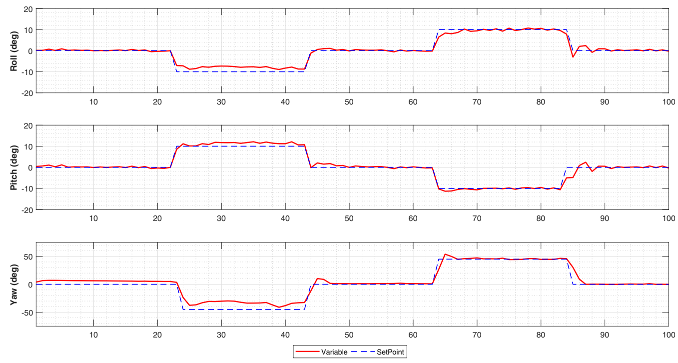

Figure 6. Angular attitude controlled responses performed in Scenario 3.

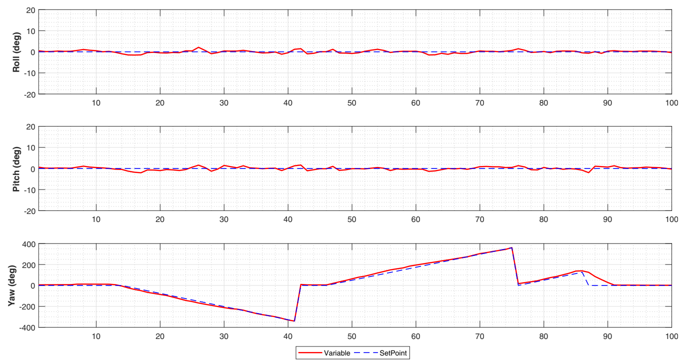

Figure 7. Angular attitude controlled responses performed in Scenario 4.

It is noted in this experimental test that the developed test bench platform also allows the UAV to perform yaw speed SPs freely. This kind of maneuver is essential to observe when considering experimental test field of image supervision onboard UAV flights.

The last video was made and uploaded on YouTube, showing its dynamics response for this scenario: https://youtu.be/WNyMbHeEmxE.

VII. Conclusions

This paper presented a safe and reliable gyroscopic test bench system to validate angular attitude of under/over actuated aircraft (respecting its constructive dimensions).

The developed system showed to be efficient when basing on experimental tests with quadrotor UAVs, avoiding possible damages to materials or injuries to people around the test area.

It is also important to mention its necessity when taking educational purposes, aiding professors to teach about this kind of aircraft dynamics.

VIII. Future Works

After concluding this work, future stages of this project can be started, such as signal estimation, design of over-actuated UAVs, development of new control loop topologies, among others.

As mentioned in Section I, signal estimation (on-line or off-line) and new controller tuning technique through decoupling can implemented using UAVs. The next step will be lead through the papers [15]–[20].

Other important works about optimization techniques to be followed are [21]–[23].

ACKNOWLEDGMENT

The authors thank INERGE, UFJF, CEFET-MG, CPFL and TBE for the financial support.

REFERENCES

[1] M. F. Santos, L. M. Honório, E. B. Costa, E. J. Oliveira, and J. P. P. G. Visconti, "Active fault-tolerant control applied to a hexacopter under propulsion system failures," in *19th International Conference on System Theory, Control and Computing (ICSTCC)*, pp. 447–453, IEEE, Oct 2015.

[2] M. F. Silva, A. C. Ribeiro, M. F. Santos, M. J. Carmo, L. M. Honório, E. J. Oliveira, and V. F. Vidal, "Design of angular PID controllers for quadcopters built with low cost equipment," in *20th International Conference on System Theory, Control and Computing (ICSTCC)*, pp. 216–221, IEEE, Oct 2016.

[3] P. Daponte, F. Lamonaca, F. Picariello, M. Riccio, L. Pompetti, and M. Pompetti, "A measurement system for testing light remotely piloted aircraft," in *International Workshop on Metrology for AeroSpace (MetroAeroSpace)*, pp. 397–402, IEEE, 2017.

[4] P. Daponte, L. De Vito, F. Lamonaca, F. Picariello, M. Riccio, S. Rapuano, L. Pompetti, and M. Pompetti, "Dronesbench: an innovative bench to test drones," *IEEE Instrumentation & Measurement Magazine*, vol. 20, no. 6, pp. 8–15, 2017.

[5] S. Alvarado, N. Certad, G. F. López, and M. González, "Construction, identification and instrumentation of a low cost quadcopter research platform," in *Latin American Robotics Symposium (LARS) and Brazilian Symposium on Robotics (SBR)*, pp. 1–6, IEEE, 2017.

[6] J. G. B. Farias Filho, C. E. Dórea, W. M. Bessa, and J. L. C. Farias, "Modeling, test benches and identification of a quadcopter," in *XIII Latin American Robotics Symposium and IV Brazilian Robotics Symposium (LARS/SBR)*, pp. 49–54, IEEE, 2016.

[7] J. Awrejcewicz, *Modeling, Simulation and Control of Nonlinear Engineering Dynamical Systems*. Springer, 2009.

[8] L. Dai and R. N. Jazar, *Nonlinear Approaches in Engineering Applications 2*. Springer, 2012.

[9] T. I. Fossen, "Mathematical models for control of aircraft and satellites," *Department of Engineering Cybernetics Norwegian University of Science and Technology*, 2011.

[10] R. W. Beard and T. W. McLain, *Small unmanned aircraft: Theory and practice*. Princeton, USA: Princeton University Press, 2012.

[11] F. C. Ferreira, M. F. Santos, and V. B. Schettino, "Computational vision applied to mobile robotics with position control and trajectory planning: Study and application," in *19th International Carpathian Control Conference (ICCC)*, IEEE, 2018.

[12] M. F. Santos, V. S. Pereira, A. C. Ribeiro, M. F. Silva, M. J. Carmo, V. F. Vidal, L. M. Honório, A. S. Cerqueira, and E. J. Oliveira, "Simulation and comparison between a linear and nonlinear technique applied to altitude control in quadcopters," in *18th International Carpathian Control Conference (ICCC)*, pp. 234–239, IEEE, 2017.

[13] V. F. Vidal, L. M. Honório, M. F. Santos, M. F. Silva, A. S. Cerqueira, and E. J. Oliveira, "UAV vision aided positioning system for location and landing," in *18th International Carpathian Control Conference (ICCC)*, pp. 228–233, IEEE, 2017.

[14] M. F. Silva, A. S. Cerqueira, V. F. Vidal, L. M. Honório, M. F. Santos, and E. J. Oliveira, "Landing area recognition by image applied to an autonomous control landing of VTOL aircraft," in *18th International Carpathian Control Conference (ICCC)*, pp. 240–245, IEEE, 2017.

[15] E. J. Oliveira, L. M. Honório, A. H. Anzai, L. W. Oliveira, and E. B. Costa, "Optimal transient droop compensator and PID tuning for load frequency control in hydro power systems," *International Journal of Electrical Power & Energy Systems*, vol. 68, pp. 345–355, 2015.

[16] L. M. Honório, A. M. L. da Silva, D. A. Barbosa, and L. F. N. Delboni, "Solving optimal power flow problems using a probabilistic α-constrained evolutionary approach," *IET generation, transmission & distribution*, vol. 4, no. 6, pp. 674–682, 2010.

[17] L. M. Honório, M. Vidigal, and L. E. Souza, "Dynamic polymorphic agents scheduling and execution using artificial immune systems," in *International Conference on Artificial Immune Systems*, pp. 166–175, Springer, 2008.

[18] L. M. Honório, E. B. Costa, E. J. Oliveira, D. de Almeida Fernandes, and A. P. G. Moreira, "Persistently-exciting signal generation for optimal parameter estimation of constrained nonlinear dynamical systems," *ISA transactions*, 2018.

[19] L. M. Honório, D. A. Barbosa, E. J. Oliveira, P. A. N. Garcia, and M. F. Santos, "A multiple kernel classification approach based on a quadratic successive geometric segmentation methodology with a fault diagnosis case," *ISA transactions*, 2018.

[20] M. M. Machado, A. J. Carvalho, M. F. Santos, and J. R. de Carvalho, "Case study: Level and temperature multivariable control and design via arduino through control loop decoupling," in *19th International Carpathian Control Conference (ICCC)*, IEEE, 2018.

[21] L. C. Gonçalves, M. F. Santos, R. J. F. de Sá, J. L. da Silva, H. B. Rezende, *et al.*, "Development of a PI controller through an ant colony optimization algorithm applied to a SMAR® didactic level plant," in *19th International Carpathian Control Conference (ICCC)*, IEEE, 2018.

[22] F. F. Panoeiro, M. F. Santos, D. C. Silva, J. L. Silva, and M. J. Carmo, "PI controller tuned by bee swarm for level control systems," in *19th International Carpathian Control Conference (ICCC)*, IEEE, 2018.

[23] J. M. S. Ribeiro, M. F. Santos, M. J. Carmo, and M. F. Silva, "Comparison of PID controller tuning methods: analytical/classical techniques versus optimization algorithms," in *18th International Carpathian Control Conference (ICCC)*, pp. 533–538, IEEE, 2017.